



A review on flow energy harvesters based on flapping foils



Qing Xiao^a, Qiang Zhu^{b,*}

^a Department of Naval Architecture & Marine Engineering, University of Strathclyde, Glasgow G4 0LZ, UK

^b Department of Structural Engineering, University of California, San Diego, La Jolla, CA 92093, USA

ARTICLE INFO

Article history:

Received 9 September 2013

Accepted 19 January 2014

Available online 3 March 2014

Keywords:

Oscillatory foil

Flow energy harvesting

Bio-inspired

ABSTRACT

This article presents an overview of the state of the art investigations on the recently developed oscillating foil energy converters. A summary of available knowledge and up-to-date progress in the application of such bio-inspired systems for renewable energy devices is provided. Starting from concepts and achieved results in three distinguishable categories, various parametric studies are reviewed, along with an in-depth discussion on the potential device performance enhancement *via* flow control mechanisms. Finally, potential future research directions are discussed.

© 2014 Elsevier Ltd. All rights reserved.

1. Introduction

In the past decade, tidal stream energy converters have become a major focus for renewable energy research, with a number of turbine farms now in planning and development. The majority of existing designs for tidal energy devices utilize either horizontal-axis or vertical-axis turbine-based energy converters. These devices, acting both singly and in arrays, present many challenges related to economic and technical viability as well as environmental impact (Westwood, 2004; Kerr, 2007; Langhamer et al., 2010).

Aquatic animals, as well as insects and birds, exploit a different kinetic mechanism in locomotion. Instead of rotational propellers, these animals utilize oscillatory motions with fins or wings to achieve highly effective propelling and maneuvering (Triantafyllou et al., 2004). For example, tuna, dolphin and shark exhibit excellent hydrodynamic performance with high cruising speed, high efficiency and low noise through the flapping motion of their caudal fins. Moreover, through these oscillatory motions it is possible to extract energy from the incoming vortices or unsteady flows. It has been numerically demonstrated that the caudal fin of a fish can absorb energy from vortices shed from dorsal/ventral fins to achieve higher propulsion efficiency (Zhu et al., 2002). A more interesting finding is that a freshly killed fish is capable of moving upstream within the Karman vortex street generated by a D-shape cylinder (Liao et al., 2003).

Bio-inspired energy harvesting devices based on the oscillatory motions of foils have been developed over several decades. An early concept is that an oscillating wing may be used to extract energy from the unsteady flow fields generated by free-surface waves (Wu, 1972; Wu and Chwang, 1975). Indeed, in both experiments and theoretical analyses it was discovered that a foil submerged right below the free surface could propel itself forward by using the energy from the incoming waves (Wu, 1972; Isshiki and Murakami, 1984; Grue et al., 1988). The application of flapping wings to extract energy from uniform flows was first proposed by McKinney and DeLaurier (1981). With the growing importance of renewable energy, the interest in this novel concept has been rekindled in the past few years. One notable phenomenon is

* Corresponding author.

E-mail address: qizhu@ucsd.edu (Q. Zhu).

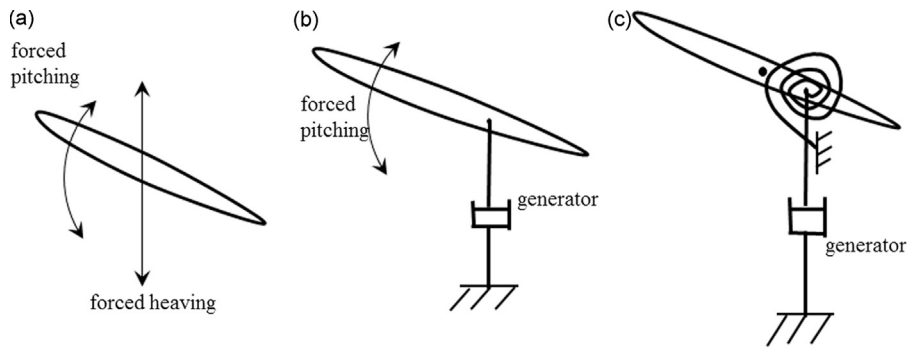


Fig. 1. Schematics of (a) a system with forced heaving and pitching motions, (b) a semi-activated system with forced pitching but induced heaving motions (modified from Zhu and Peng (2009)), and (c) a self-sustained system with induced heaving and pitching motions (modified from Peng and Zhu (2009)).

the involvement of industry in developing full-scale prototypes, including, e.g. the *Oscillating Marine Current Energy Converter* initially developed by *The Engineering Business Ltd.* (The Engineering Business Ltd. Technical Reports, 2002, 2003, 2005) and further improved by *Pulse Tidal Ltd.* (<http://www.pulsetidal.com>).

Unlike conventional turbines, there are several prominent features of such bio-inspired energy converters: (i) they are environmentally friendly in terms of noise generation due to their relatively low tip speed, thus reducing impact on the navigation of aquatic animals; (ii) without the centrifugal stress associated with rotating blades, the oscillatory devices are structurally robust; (iii) oscillating hydrofoil systems sweep a rectangular cross section of flow. The swept area for a single device can thus be wide and shallow, allowing large systems to be installed in shallow water. Subsequently, multi-megawatt devices can be envisaged for a wider range of tidal stream resource areas.

With the rapid development of such devices, the understanding of their underlying physics, including the fluid dynamics, the fluid–structure interactions, and the coupled dynamics of the nonlinear system, is required in order to improve the existing devices' efficiency and pave the way for the development of new systems that will be commercially profitable. In the past few years, the research on the dynamics of oscillating energy extraction devices based on flapping foils has attracted gradually more attention, as demonstrated by the increasing number of publications. A broad review of the relevant literature is timely and necessary.

Despite the apparent similarity between flapping foil flow energy harvesters and flapping foil propellers (which have been studied extensively), there exist key differences between them. For instance, in the propeller the energy flux is from the foil to the fluid, whereas in the harvester it is in the opposite direction. In addition, the wake behind the propeller is of the thrust type (reverse Karman Vortex Street) and the one behind the harvester is of the drag type. This suggests different stability properties of the wakes, and subsequently, different features in wake–body interactions. Finally, the performance of the propeller is characterized by the longitudinal thrust it generates. For the harvester, on the other hand, the performance is determined by the magnitudes and phases of the lifting force and the pitching moment.

The goal of this paper is to review studies that have contributed to our understanding about the behavior of oscillating foil energy harvesters, and to provide guidelines for possible research directions in the near future. The structure of this review article is described as following. We begin with a brief description of the three basic designs of oscillating wing energy harvesting devices that have been proposed in the literature. This is followed by the review of the existing studies about the dynamical characteristics of each of them. The concentration will be on the fluid dynamics mechanisms that contribute to enhanced performance in energy extraction, including, e.g., the parametric studies, the correlation between energy harvesting performance and wake instability, and requirements to achieve periodic flapping in a self-sustained system. Finally, we will summarize remaining issues and explore possible research directions in the future.

2. Basic designs of flapping foil flow energy harvesters

The studies on flapping type energy converters can be classified into the following three categories with respect to the activating mechanism of the device.

2.1. Type 1: systems with forced pitching and heaving motions

As shown in (Fig. 1a), these systems feature prescribed pitching motion $h(t)$ and heaving motion $\theta(t)$. Obviously, without taking into account the actuation mechanism they are mostly hypothetical. However, these idealized models are simple and easier to formulate mathematically, and thus are favoured in existing theoretical and numerical studies. The results obtained can provide some useful theoretical insights and guidance for real devices design at preliminary stage. Due to the specified pitching and heaving motion, the power generation for Type 1 device equals the sole available aero-/hydro-dynamic power input into the system. If the motions are periodic with time period T , the energy harvesting performance is often

characterized by the cycle-averaged power coefficient (C_{op}) defined as

$$C_{op} = \bar{P} / ((1/2)\rho U_{\infty}^3 cs), \quad (1)$$

where U_{∞} is the speed of the incoming flow, ρ is the fluid density, c is the chord length of the foil, s is the span length, and \bar{P} is the cycle-averaged power given as

$$\bar{P} = \frac{1}{T} \int_t^{t+T} [Y(t)\dot{h}(t) + M(t)\dot{\theta}(t)] dt, \quad (2)$$

where $Y(t)$ and $M(t)$ are instantaneous lifting force and pitching moment, respectively. A more illustrating measure of performance is the efficiency of energy harvesting, defined as the portion of incoming flow kinematic energy flux extracted by the system, which is mathematically expressed as

$$\eta = \bar{P} / (1/2)\rho U_{\infty}^3 Y_p s, \quad (3)$$

where Y_p is the difference between the highest and the lowest points reached by the foil.

2.2. Type 2: systems with forced pitching and induced heaving motions (semi-activated systems)

These systems require controlling/actuating the pitching motion (Fig. 1b). The existing flapping type energy harvesters in industry are often based on this design. Hereby energy input is needed to activate the pitching motion, whereas energy harvesting is achieved through the resulting heaving motion generated by fluid dynamic lifting forces. Positive net energy extraction is possible only if the energy extracted from the heaving motion is higher than the energy expenditure to activate the pitching motion. If the energy extractor is idealized as a linear damper with damping coefficient c_0 , the net power extraction is expressed as

$$\bar{P} = \frac{1}{T} \int_t^{t+T} [c_0 \dot{h}^2(t) - M(t)\dot{\theta}(t)] dt. \quad (4)$$

2.3. Type 3: systems with self-sustained pitching and heaving motions (self-sustained systems)

These systems rely on flow-induced instabilities to generate oscillatory motions in the heaving and pitching directions (Fig. 1c). This greatly simplifies the mechanical design since no actuation system is needed. The subsequent energy extraction, *per se*, is guaranteed to be positive. If the motions are periodic (with period T), and we only consider energy extraction from the heaving motion, the corresponding net power extraction is

$$\bar{P} = \frac{1}{T} \int_t^{t+T} c_0 \dot{h}^2(t) dt. \quad (5)$$

The efficiency for Type 2 and 3 systems follow the same definition as shown in Eq. (3). It should be pointed out that the net powers obtained by Eqs. (2), (4), and (5) refer to the upper limit of the power harvesting capacity without considering the efficiencies of the mechanical system and the electricity generating system.

In the following, we conduct detailed reviews of existing studies on these three types of design in separate sections. A detailed list of the representative studies is summarized in Appendix A.

3. Review on systems with forced pitching and heaving motions

In this category, a foil is forced to oscillate with prescribed plunging (heaving) and pitching motions. In most of the existing studies, it was assumed that the foil undergoes sinusoidal motions in both heaving and pitching directions so that $h(t) = h_0 \sin(\omega t)$ and $\theta(t) = \theta_0 \sin(\omega t + \varphi)$.

To describe this problem quantitatively, there are several kinematic parameters, including oscillating amplitudes (h_0 and θ_0), frequency (ω or $f = \omega/2\pi$), and the phase lag between heave and pitch motion (φ). Among them, two forms of non-dimensional frequency are adopted by most researchers, reduced frequency ($f^* = fc/U_{\infty}$) and Strouhal number ($St = 2fh_0/U_{\infty}$). We present a literature review about the influences of these kinematic parameters on the power extraction performance.

3.1. Effects of kinematic parameters

As mentioned in the Introduction, the study of flapping foil flow energy harvester started with the experimental work by McKinney and DeLaurier (1981), which proved the feasibility of flow energy extraction by a harmonically oscillating wing. Following that idea, Jones and Platzer (1997) examined the transition from thrust generation to power extraction by using an unsteady panel code coupled with a boundary layer algorithm. By fixing the plunging amplitude, frequency and amplitude (at 0.2c), they demonstrated that if the pitching amplitude was increased to a sufficiently high value, the

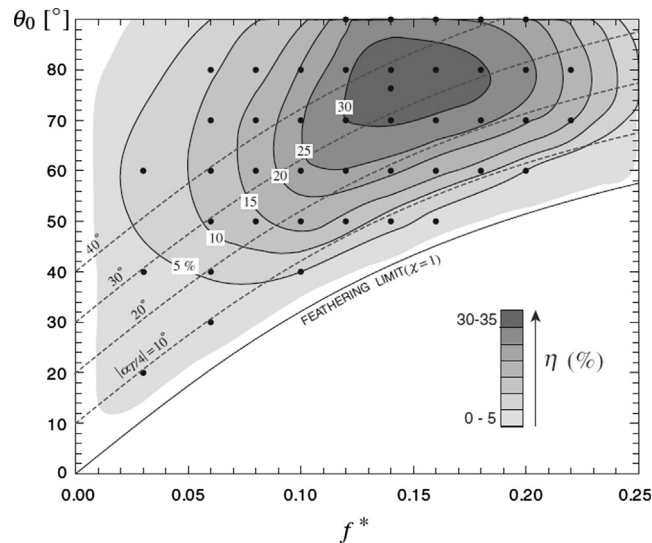


Fig. 2. Mapping of efficiency (η) in the parametric space (f^* , θ_0) (flapping frequency, pitching amplitude) for a NACA0012 at $Re=1100$. The heaving amplitude equals the chord length, and the pitching axis is located at $1/3$ chord length from the leading edge. The simulated cases are shown with black dots and iso-efficiency contours are sketched approximately (Kinsey and Dumas, 2008).

oscillating wing system switched from propulsive mode to energy extraction mode. With various combinations of pitching and plunging motions, the condition for power extraction occurrence is that the pitching amplitude (θ_0) must exceed the plunging-induced angle of attack ($\arctan[\dot{h}(t)/U_\infty]$). A feathering state is reached when the heave-induced angle of attack equals the pitching angle. At this state, the oscillating wing generates neither thrust nor drag.

Ever since these pioneering studies, an important focus of the following work has been to identify the optimal combination of kinematic parameters that lead to the best performance of the system (hereby the system performance is usually quantified using the energy harvesting efficiency defined in Eq. (3)), so that this novel system can compete with the traditional designs based on rotating blades.

With both experimental measurements and numerical simulations using an unsteady panel code, the results obtained by Davids (1999) show that the efficiency of energy extraction with an oscillating NACA0012 foil can reach 30% with optimized combination of plunging amplitude and frequency. More systematic numerical and experimental investigations were carried out by Lindsey (2002) on a twin-wing system and Jones et al. (2003) on a single-wing system. Recent computational efforts by Dumas and Kinsey (2006) and Kinsey and Dumas (2008) present a mapping of energy-extraction efficiency for an oscillating NACA0015 foil in the frequency and pitching amplitude domain (Fig. 2). Through unsteady laminar-flow simulations using the commercial software FLUENT, they observed that within the domain of $0 < f^* < 0.25$ and $0 < \theta_0 < 90^\circ$, the maximum efficiency could go up to 34% when the plunging amplitude is around one chord length and the pitching axis is located at one third of the chord length from the leading edge.

For a single oscillating wing, the influence of oscillating frequency, heaving amplitude, pitching amplitude and phase lag between heave and pitch on the power efficiency are summarized as follows.

3.1.1. Oscillating frequency

The influence of oscillating frequency on the variation of power extraction efficiency of a flapping foil energy harvester is very similar to that of a flapping foil propeller. Specifically, when other parameters are fixed, the energy extraction efficiency initially increases monotonically with frequency f^* . After reaching a peak, it decreases sharply when f^* is further increased. Locally, the peak frequency depends on other kinematic parameters, such as the amplitudes of pitch and heave, phase lag between pitch and heave, and even the pivot point for pitching motion. However, the global optimal point corresponding to the peak efficiency at all possible combinations of parameters always occurs when the reduced frequency f^* is within the range between 0.10 and 0.15. Physically, this has been explained as the point at which the most unstable disturbance mode at the wake is triggered (Zhu, 2011). A detailed description about this work is provided later.

3.1.2. Heaving amplitude

As we discussed earlier, to reach an energy extraction state the angle of attack induced by heaving must be smaller than the pitching amplitude. To achieve sufficient power output, the heaving amplitude (h_0) is usually chosen to be comparable to the chord length. Given that the other parameters are fixed, the general observations from relevant studies are that as the heaving amplitude increases, the power coefficient (C_{op}) increases linearly (Davids, 1999; Lindsey, 2002; Dumas and Kinsey, 2006; Xiao et al., 2012). However, this trend is not always true for the efficiency η . In fact, the effect of heaving amplitude on η is intricate since it affects not only the oscillating velocity but also the size of the wing swept area. According to these

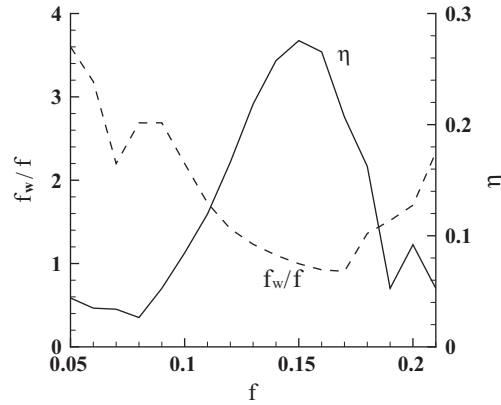


Fig. 3. The most unstable wake frequency f_w and the energy harvesting efficiency η at different oscillatory frequencies of a flapping foil (Zhu, 2011). The frequencies are normalized by the incoming flow speed and the chord length. The heaving amplitude equals half chord length, and the pitching amplitude is 90° .

studies, at low plunging amplitudes ($h_0 < 0.5c$), η increases significantly with h_0 . Once the plunging amplitude reaches one chord length, the efficiency drops since the swept area continues to grow while the angle of attack at certain parts of the oscillating cycle is reduced.

3.1.3. Phase lag between pitch and heave

Within the range of variables, it is found that peak energy extraction occurs when the pitch and plunge motions are 90° out of phase (Davids, 1999; Dumas and Kinsey, 2006; Kinsey and Dumas, 2008). There might be some variations if the pivot point moves downstream from one third (or one quarter) of chord length to half of chord length from the leading edge.

3.1.4. Effective angle of attack (AoA)

The dynamics of the system is determined by the combination of kinematic parameters so that they often need to be considered in an integrated way. One parameter commonly adopted by researchers in the flapping wing propulsion study is the ‘effective angle of attack’ defined as

$$\alpha_{eff}(t) = -\arctan\left[\frac{\dot{h}(t)}{U_\infty}\right] + \theta(t). \quad (6)$$

The nominal angle of attack (α_0), which is not time independent, is widely adopted in the flapping foil studies. It is defined as

$$\alpha_0 = -\arctan\left(\frac{\omega h_0}{U_\infty}\right) + \theta_0. \quad (7)$$

For convenience, sometimes α_0 is also called ‘effective AoA’. As indicated in its definition (Eq. (7)), this parameter combines the contributions of pitch, heave, oscillating frequency, as well as the incoming flow conditions. Similar to the flapping wing for propulsion purposes, studies on the impact of effective AoA reveal a trend of power (efficiency) increase with the increasing α_0 when its value is low (Davids, 1999; Xiao et al., 2012).

Although the effective AoA is more physically relevant due to its close correlation with leading edge separation (Zhu, 2011), in most existing experimental investigations the pitching amplitude (rather than the effective AoA) was utilized as a characteristic parameter (Jones and Platzer, 1997; Jones et al., 2003; Dumas and Kinsey 2006; Kinsey and Dumas, 2008; Simpson et al., 2008a,b; Ashraf et al., 2011).

3.1.5. Location of the pitching axis (pivot location)

For most oscillating foils in aerodynamic or hydrodynamic applications, the pitching axis is located at one third or one quarter chord length from the leading edge. This mitigates the energy expenditure to generate the pitching motion since the center of fluid force is roughly at the quarter chord point. It has been illustrated that in flapping foil energy harvesters adjusting the pivot location has a similar effect as changing the phase lag between pitch and heave (Davids, 1999; Kinsey and Dumas, 2008). Indeed, a systematic study by Davids (1999) on the relation between phase lag and pivot point shows an obvious interdependency. For phase lag less than 90° , the pivot point corresponding to maximum C_{op} exits in the aft of mid-chord. However, for phase lag greater than 90° , the optimum pivot location moves forward towards the leading edge. A subsequent investigation on the analysis of instantaneous vortex shedding and pressure distribution on the foil surface shows that changing the pivot point of the foil directly modifies the instantaneous local acceleration of the body surface, leading to modified vorticity fluxes at the wall (Kinsey and Dumas, 2008). The general conclusion drawn from these studies

is that the highest efficiency occurs when the pivot is just in front of the mid-chord position. This can be attributed to the foil's effective thickness related to the occurrence of dynamic stall.

3.2. Effect of wake instability on the flow energy harvesting efficiency

It is well understood that the propulsive efficiency of a flapping foil propeller is closely related to the flow instability property in its wake. The wake behind a flapping foil is found to be convectively unstable. In this scenario, disturbances grow as they travel downstream, whereas no local growth is possible. It was also found that the maximum propulsive efficiency coincides with the triggering of the most unstable modes in the wake at an optimal Strouhal number of around 0.3 (Triantafyllou et al., 1991, 1993). The explanation is that an efficiently generated reverse Karman vortex wake directly contributes to high-efficiency thrust generation. In this sense, the flapping foil energy harvester is similar since its energy harvesting performance is also related to the strength of its wake. Hereby the flow energy recovery capacity is determined by the velocity reduction in the wake, which is induced by vortices shed from the foil.

A numerical study has been conducted to examine the correlation between wake instability and energy harvesting performance of a flapping foil (Zhu, 2011). This work involves prescribed (sinusoidal) heave and pitch motions of a two-dimensional foil. The fluid dynamics is solved by using a Navier–Stokes solver. The most unstable modes have been identified by solving the inviscid Orr–Sommerfeld equation, in which the base flow (the time-averaged flow in the wake) is obtained numerically with that N–S solver. The key finding is that the highest energy extraction efficiency is achieved when the flapping frequency coincides with the frequency of the most unstable mode (see Fig. 3). This scenario can only occur with significantly strong vortex generation from the leading edge, which is triggered by large effective angles of attack ($> 40^\circ$). The corresponding reduced frequency f^* is in the range between 0.10 and 0.15, consistent with previous studies.

3.3. Other parametric effects

3.3.1. 3D effect

In real operations, the wing always has limited aspect ratio so that the end effect due to finite-length wingspan may affect its performance. Studies on the three-dimensional effect have been performed by Simpson et al. (2008a,b) and Kinsey and Dumas (2012c).

With a water tank testing and force/load measurement for a NACA0012 hydrofoil at three different aspect ratios (AR=4.1, 5.9, and 7.9), the results from Simpson et al. (2008a,b) show a clear decrease of efficiency as AR decreases. According to this study, the high efficiency around 40% is only present in the high aspect ratio foil. This is reminiscent of flapping foil propellers, which demonstrates the same trend. A peak efficiency of 43% was found at the aspect ratio of 7.9, the Strouhal number of 0.4, the maximum angle of attack of 34.37° , and the phase difference between pitching and plunging of 90° .

A numerical study about the three-dimensional effect was carried out by Kinsey and Dumas (2012c) for two aspect ratios, 5.0 and 7.0. Similar to the experimental work of Simpson et al. (2008a,b), their simulations demonstrated that the maximum cycle-averaged power of finite AR wings is lower than that of a two-dimensional wing. Given the flow and flapping conditions of Reynolds number $Re=500\,000$, reduced flapping frequency $f^*=0.14$, pitching amplitude $\theta_0=75^\circ$, and heaving amplitude $h_0=c$, the peak energy harvesting efficiency is 28% for AR=7.0, and drops to 21% for AR=5.0. Detailed examination on the vorticity field along the 3D wingspan over a cycle indicates a remarkable difference between 2D and 3D wings at those instants when strong vortex shedding occurs. Similar to a 2D wing, an enlarged vortex evolves and sheds at the mid-span of a 3D wing (Fig. 4), which leads to a significant difference between the pressure distributions on the top and bottom wing surfaces. This results in instantaneous lift force and moment augmentation, and enhances energy harvesting efficiency. However, such vortex generation process is weakened near the wingtip areas. As a result, the three-dimensional effect smoothens out the influence of vortex and reduces the peak of the instantaneous force. On the other hand, at the instants when the boundary layer remains attached, no pronounced difference in flow structure and pressure distribution is observed between 3D and 2D wings.

3.3.2. Foil shape effect

Most of the existing studies are based on NACA 00 series foils (including NACA0002, 0010, 0012, 0014, 0015, 0018 and 0020). Some brief studies have been done to examine if the foil thickness might have any impact on the power generation efficiency. With a panel method, the numerical work by Lindsey (2002) showed that the foil thickness did have an effect if the flow stays attached to the air foil. It appears that a thinner foil can enhance performance. However, since an inviscid flow model was adopted, in his study the flow separation due to viscous effect was ignored. This is believed to affect the accuracy of the conclusion. To overcome this issue, an investigation with a viscous Navier–Stokes solver was performed by Dumas and Kinsey (2006). They found that the overall efficiency, as well as the occurrence of dynamic stall, was not sensitive to the foil geometry. Similar results were observed in their follow-up study (Kinsey and Dumas, 2008). In particular, though the details of leading vortex shedding, shear layer rolling up, and instantaneous forces are different among the three investigated foils (NACA0002, 0015 and 0020), the time-averaged efficiency remains almost unchanged.

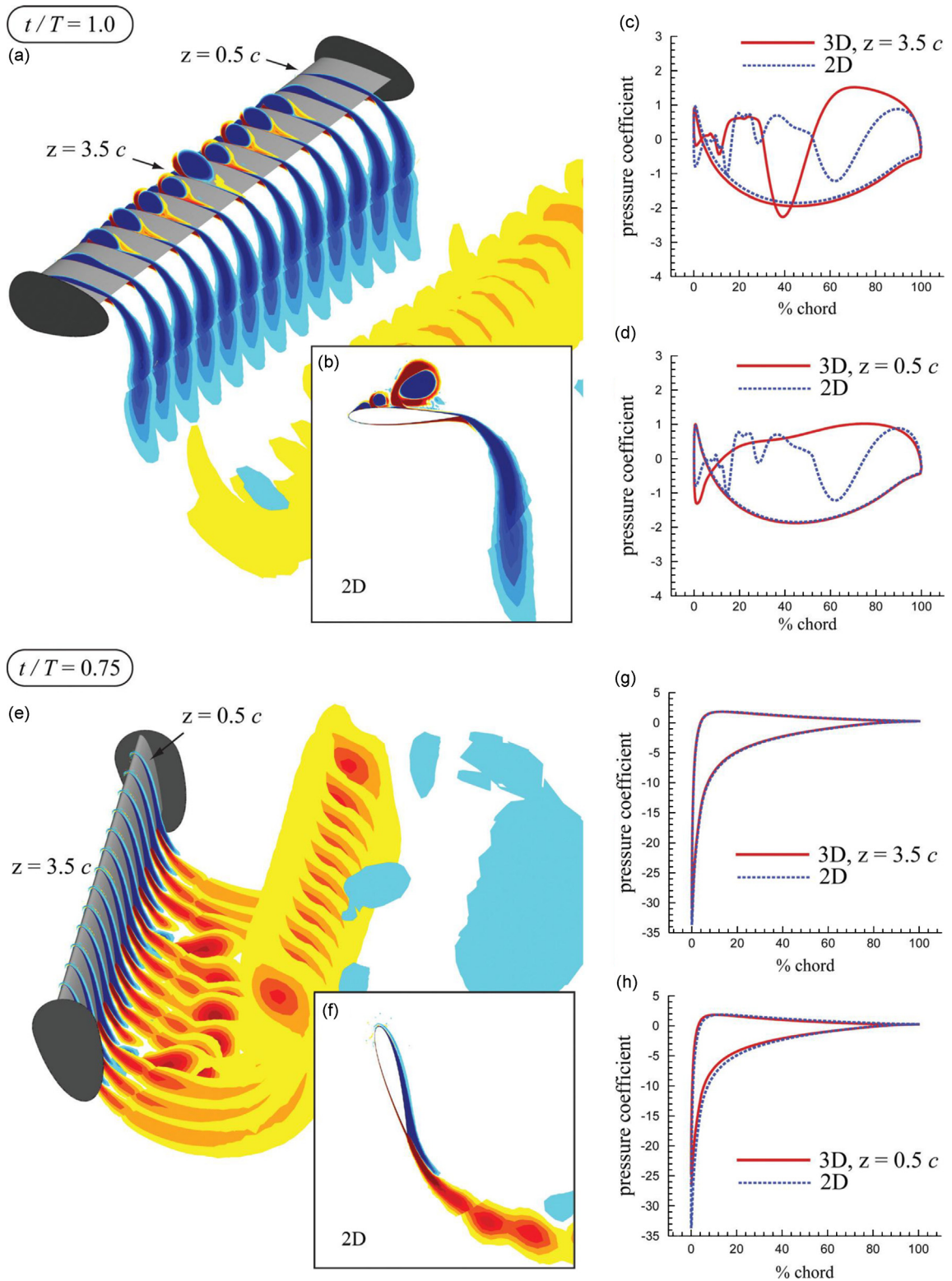


Fig. 4. Comparison between 2D and 3D (AR=7) predictions at two instants during the cyclic motion of the foil. Flow structures are visualized using slices of Z-vorticity at every half-chord length distance along the foil span (blue for negative vorticity and red for positive) (Kinsey and Dumas, 2012c). Pressure coefficient distributions along the chord line are provided and compared to 2D results for two stations along the span; one at midspan ($z=3.5c$) and one at only $0.5c$ away from the wingtip. (For interpretation of the references to color in this figure legend, the reader is referred to the web version of this article.)

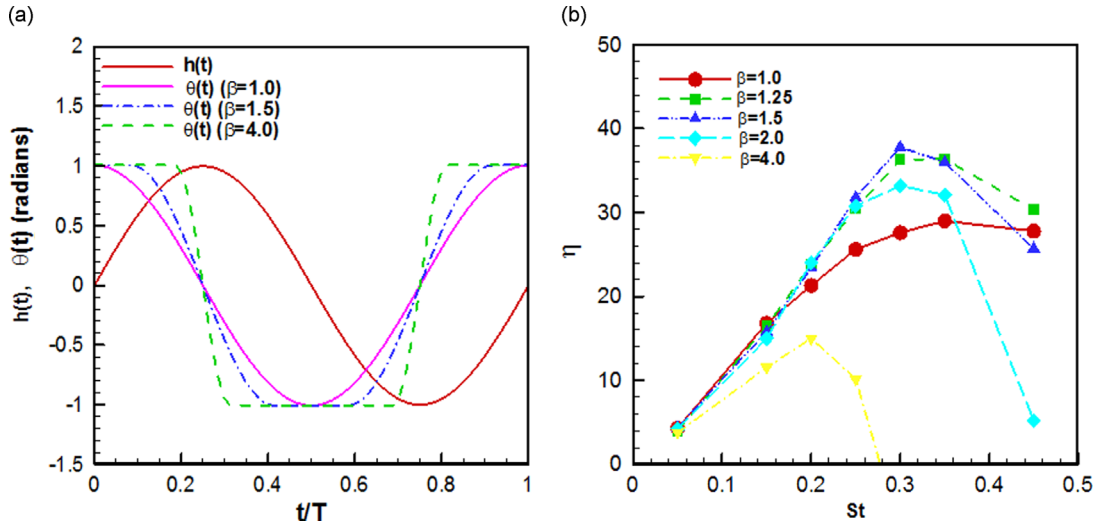


Fig. 5. The influence of non-sinusoidal pitching profiles on oscillating wing power efficiency: (a) Profile of pitching and heaving with an adjustable constant β ; (b) efficiency variation with β at various oscillating non-dimensional frequency St (heaving and nominal effective angle of attack $h_0/c=1.0$ and $\alpha_0=20^\circ$) (Xiao et al., 2012).

3.3.3. Reynolds number effect

In real applications, the energy harvesting devices usually work in Reynolds numbers much higher than those considered in numerical simulations and laboratory experiments. Studies on the effect of Reynolds number are thus critical in bridging the gap between existing studies and future applications. In the early days, Lindsey (2002) and Jones et al. (2003) conducted simulations with Navier–Stokes solvers to predict the influence of Reynolds number. Considerably higher power efficiency was observed over a range of reduced frequency between 0.2 and 1.2 when the Reynolds number increases from 2×10^4 to 10^6 . This suggests that the presence of large flow separation due to dynamic stall at high Re is beneficial to energy extraction. A more detailed investigation in this aspect has been done by Dumas and Kinsey (2006) and Kinsey and Dumas (2008). Assuming laminar flow condition, a preliminary study by Dumas and Kinsey (2006) was focused on two Reynolds numbers ($Re=500$ and 2400). They found that the efficiency increased slightly with Reynolds number. The reduced viscous diffusion at high Re is likely to reduce the effective thickness of the wing and increase the force generation. Further studies by Kinsey and Dumas (2008) concluded that energy harvesting efficiency increased from 32.7% to 36.4% when Re rises from 500 to 10 000.

Numerical simulations based on an unsteady Reynolds averaged Navier–Stokes solver at even higher Reynolds numbers in the turbulent regime requires the proper selection of turbulence models. It is well known that the prediction of flow separation and reattachment point varies profoundly with different turbulence models when massive separations occur. A test was performed by Kinsey and Dumas (2012a) with various available turbulence models embedded in the commercial software FLUENT, including 1-equation Spalart–Allmaras model, 2-equation $k-\omega$ standard, $k-\omega$ SST, and $k-\omega$ SST (low Re correction) models for a single oscillating wing at $Re=5 \times 10^6$, $f^*=0.14$, and $\theta_0=75^\circ$. Surprisingly, the predicted instantaneous force and power efficiency from different turbulence models agree closely with only one percent difference in efficiency (38–39%). However, a further comparison between simulation results with S–A model and experiment shows that the model predicts the efficiency very well at low frequencies ($f^* < 0.08$), but over predicts the efficiency for $f^* \geq 0.08$. This is likely attributed to the enlarged separation regions at high f^* . Oscillating foil study within the turbulent flow regime has also been conducted by Liu et al. (2013) with 2-equations $k-\omega$ turbulence model for single and twin wings.

3.4. Mechanisms to further enhance energy extraction capacity

Leading edge vortex (LEV) generation and shedding are believed to play a significant role in power generation. Specifically, the timing of LEV shedding is critical to maximize the power extraction efficiency via varying the local surface pressure distribution (Kinsey and Dumas, 2008; Zhu and Peng, 2009). Referring to the power coefficient definition in Eqs. (1) and (2), there are four major aspects influencing the power extraction level: (a) magnitude of the vertical force $Y(t)$, (b) magnitude of the heaving velocity $\dot{h}(t)$, (c) the synchronization between $Y(t)$ and $\dot{h}(t)$ as well as the synchronization between the pitch moment $M(t)$ and the pitch velocity $\dot{\theta}(t)$, and (d) the relative contribution of pitch ($M(t)\dot{\theta}(t)$) and heave ($Y(t)\dot{h}(t)$) in one oscillating cycle. To achieve maximum performance, apart from a higher favorable heaving amplitude, $Y(t)$ and $\dot{h}(t)$ (as well as $M(t)$ and $\dot{\theta}(t)$) have to be of the same sign within most of the cycle to avoid occurrences of negative power. In addition, the following mechanisms have been explored to enhance the energy harvesting performance.

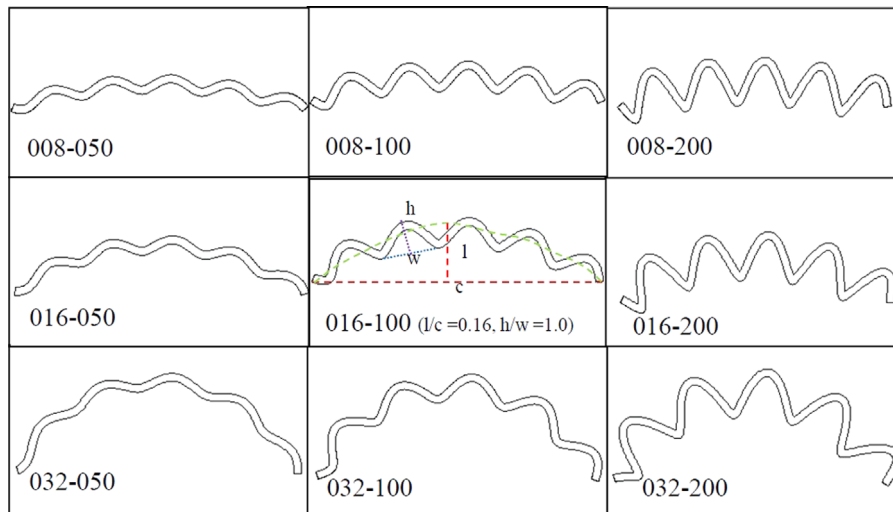


Fig. 6. A biomimetic foil shape imitating scallop shell (Le et al., 2013). The number constituting the model name refers to the percent of camber and corrugation. For instance, 016–100 means 16% of the camber with a ratio of height to the width of local corrugation at 1.0.

3.4.1. Non-sinusoidal motion

Most investigations on the kinematic parameters effect on energy harvesting efficiency are based on sinusoidal motions, which are the most fundamental harmonic profile for a flapping motion. However, in nature, the high propulsion efficiency of flying and swimming animals might be achieved by non-sinusoidal locomotion trajectories (see for example Licht et al., 2010). Inspired by this biological mechanism, the influence from non-sinusoidal oscillation motions has been studied (Platzer et al., 2010; Ashraf et al., 2011; Xiao et al., 2012). Platzer et al. (2010) and Ashraf et al. (2011) investigated a series of non-sinusoidal motions with a fixed frequency $f^* = 0.8$, heaving amplitude of $1.05c$, and pitching amplitude of 73° . For a single NACA 0014 foil undergoing non-sinusoidal pitch–plunge motion, their results indicate around 17% increase in power generation and around 15% increase in efficiency over those with sinusoidal motions. Following these studies, a more comprehensive work was performed by Xiao et al. (2012) with systematic variations of flapping frequency ($0.05 < St < 0.5$), nominal effective angle of attack ($10^\circ < \alpha_0 < 20^\circ$), and plunging amplitude ($0.5c < h_0 < c$). A trapezoid-like pitching profile was investigated, with the portion of flattened pitching angle ($\theta = \pm \theta_0$) within each oscillating cycle being adjustable via a parameter β . Their numerical simulations for a NACA0012 foil showed that the benefits on the efficiency enhancement from non-sinusoidal profile relied considerably on β as well as the other kinematic parameters (Fig. 5). For a given nominal effective angle of attack α_0 and plunging amplitude h_0 , there exists an optimal β at which the power output significantly increases. This investigation also shows that over a wide range of St , there exists an optimal pitching profile which may increase the output power coefficient and efficiency by as much as 63% and 50%, respectively.

3.4.2. Corrugated foils

Biomechanical studies on the surface pattern of a dragonfly wing indicate that a corrugated structure with various ‘tabulators’ on it can enhance the aerodynamic performance via increased lift and reduced drag (see for example Kesel, 2000). The unsteady vortices generated inside valleys formed by the pleats effectively control the flow separation size by changing the laminar boundary layer to a turbulent one. Similar designs are found in other living systems (e.g. scallop shells). Inspired by this biological concept, new models with corrugated foils have been proposed (Fig. 6) (Le et al., 2013). Their numerical simulations showed that the detailed profile of the foil played a role in controlling the vortex generation location, timing and velocity, and its performance in energy generation. An optimized foil shape with corrugation and camber was found to improve the efficiency by around 6% as compared to the NACA0012 profile. A further improvement as much as 17% is possible if the convex surface meets a free flow during both up and down strokes.

3.4.3. Structural flexibility

Structural flexibility is known to have beneficial effects on the performance of flapping foils in force generation. For example, previous studies on insect wings and fish fins suggest that certain degree of flexibility may lead to the generation of higher thrust or lift forces. This is attributed to the structural resonance, the manipulation of the LEV generation, and the force reorientation effect associated with the deformations (Katz and Weihs, 1978; Zhu, 2007; Michelin et al., 2009; Yin and Luo, 2010; Massoud and Alexeev, 2010; Thiria and Godoy-Diana, 2010; Ramananarivo et al., 2011; Shoele and Zhu, 2013). On the other hand, the effect of structural flexibility on the performance of flapping wing energy harvesting devices is not fully understood. In order to study the role of structural flexibility in the hydrodynamics of flapping wing energy devices, Liu et al. (2013) computationally modeled two-dimensional flexible flapping wings operating within the energy extraction regime. Rather than directly solving the coupled fluid–structure interaction problem, the flexible motion is pre-determined based on priori structural results. Four different

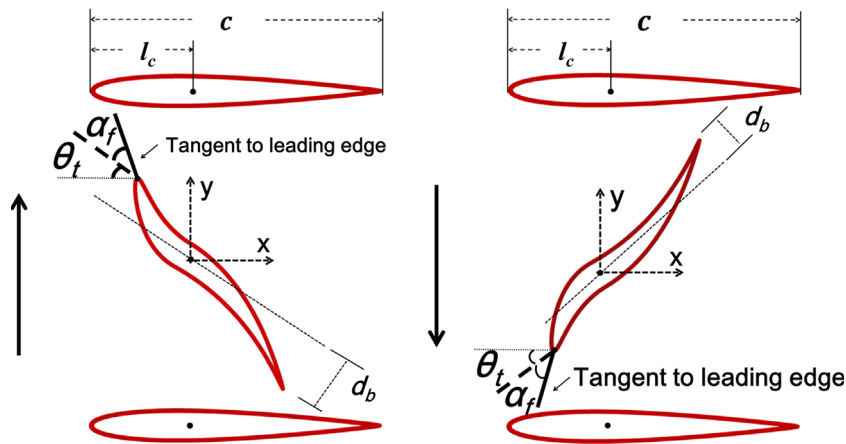


Fig. 7. An energy harvester with a flexible foil, emulating the hawkmoth wing (trailing edge control) and the trout ray fin (leading edge control) (Liu et al., 2013).

models are investigated with concentrated deformations near the leading and trailing edges, as shown in (Fig. 7). Their simulation results show that the flexibility of a wing is potentially beneficial to energy harvesting by increasing the peaks of lift force over a flapping cycle and tuning the phase shift between force and velocity towards a favorable trend. The impact of wing flexibility on efficiency is more profound at low nominal effective angles of attack. At a typical flapping frequency $f^* = 0.15$ and nominal effective AoA of 10° , a flexible wing delivers 7.68% higher efficiency than a rigid wing. An even higher increase, around six times that of a rigid wing, is achievable if the nominal effective AoA is reduced to 0° at feathering condition. A closely related study is a flexible plate flow energy harvester inspired by fluttering flags (Tang et al., 2009; Doaré and Michelin, 2011; Michelin and Doaré, 2013). Energy harvesting is achieved through piezoelectric devices attached to the plate. Unlike the flapping foils, in these cases the energy extraction depends solely upon the flexibility of the plate.

3.4.4. Multiple-foil configurations

In nature, fish swim in schools and birds fly in flocks to save energy expenditure through interactions between neighbors (see for example Belyayev and Zuyev, 1969). Previous studies on live fish or tandem/parallel oscillating foil propellers have proven that, with a proper distance between two adjacent foils, the energy of previously shed vortices can be effectively utilized to increase the thrust generation (e.g. Zhu et al., 2002; Deng et al., 2007). In practice, a similar principle is adopted by commercial wind farms in which multiple wind turbines in either tandem or parallel configurations are often used. It is thus natural to investigate the application of multiple foil arrangements in flow energy harvesting. In such a system, additional parameters such as the distances and phase differences between neighboring foils have to be considered. The earlier experiments of Lindsey (2002), Jones et al. (2003), and Platzer et al. (2010) suggested that the power generation capacity might be increased by using two foils oscillating in a tandem arrangement. This is based on experimental tests in water tunnels. The stream-wise separation between the two foils is $X = 9.6c$ and the phase lag ϕ_{1-2} is 90° . A more detailed numerical investigation was conducted by Ashraf et al. (2011) to examine the impact of varying the distance and phase difference between two NACA0014 foils pitching at $1/2$ chord length at Reynolds number of 20 000, reduced oscillating frequency of 0.8, heave amplitude of $1.05c$, and pitch angle of 73° . Their study covers three distances ($X = 2.0c, 4.0c,$ and $6.0c$) and three phase lags ($\phi_{1-2} = 0^\circ, 90^\circ,$ and 180°). The results show that both phase lag and distance have profound impact on the energy harvesting capacity and efficiency. To achieve an enhanced power output, the downstream wing must locate at an optimal place in the vortex wake of the upstream wing. Such an optimal distance varies with the phase difference between the two foils as well as the flow speed. Within the parameter range they covered, it is found that in the tandem arrangement both averaged power output and efficiency *per foil* are reduced by around 20% compared with a single foil. However, the overall efficiency of the tandem configuration is increased by up to 59% compared to that of a single foil. Hereby the overall efficiency of a multi-foil system is defined using Eq. (3), in which the time-averaged power \bar{P} is calculated as $\bar{P} = \sum_i \bar{P}_i$, where \bar{P}_i is the averaged power of each individual foil. In a tandem configuration, the overall system sweeping area is the same as that of an individual foil, whereas the sweeping area of a parallel configuration represents the area swept by the whole system, which is different from that of a single foil.

Lefrançois (2008) investigated the power extraction performance of a dual-foil turbine in both parallel and tandem configurations. Using an in-house Lagrangian vortex method, low-Reynolds ($Re = 1100$) numerical simulations were performed. It was found that in a tandem configuration, a power extraction efficiency of 41% was reached by two oscillating flat plates ($0.15c$ thickness) with six chord lengths apart from each other and a phase lag of 180° at a reduced frequency of 0.12. For a pure parallel configuration, the maximum efficiency is 31%.

A recent study by Kinsey and Dumas (2012a,b,c) demonstrated again that the relative positioning of the downstream foil oscillating in the wake shed by the upstream foil is critical to maximize the energy extraction efficiency of the device. Within the parameter range tested, both the upstream and the downstream foil achieved a higher efficiency than a single

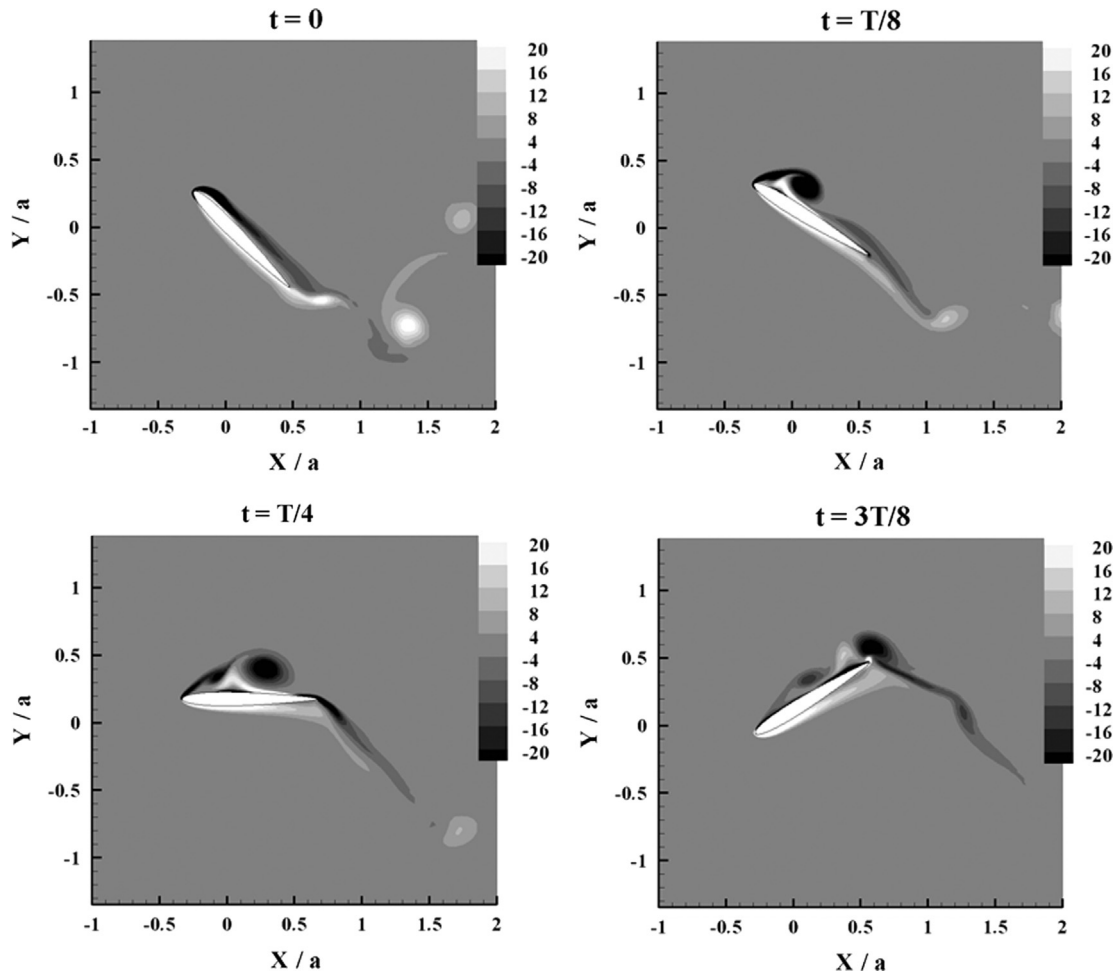


Fig. 8. A vortex-control mechanism that can enhance flow energy harvesting. Hereby due to the synchronization between foil motion and wake evolution, the direction of the pitching moment induced by the LEV coincides with the pitching motion so that the energy of the LEV is partially recovered (Zhu and Peng, 2009).

one. The contribution of downstream foil to the overall energy extraction depends very much on the interactions between upstream and downstream foils. An unfavorable interaction may even cause the downstream foil to contribute negatively to the energy extraction.

Accompanying their numerical simulations, a prototype of a tandem-foil energy harvester has been created by Kinsey et al. (2011). This system consists of two foils that are mechanically coupled – the heaving motion of one foil is coupled with the pitching motion of another. A single motor/generator is installed, which acts as a motor during portions of a cycle when energy input into the system is needed, and a generator when positive energy harvesting is achieved. The results obtained by experiments and simulations are comparable with each other.

Apart from the above findings, a global phase shift parameter was introduced to better characterize the tandem configuration. This parameter (ϕ_{1-2}) combines the spacing (L_x) and the phase lag (ϕ_{1-2}) as $\phi_{1-2} = 2\pi(L_x/U_\infty T) + \phi_{1-2}$, where T is the period of flapping. Simulation results show that different cases present similar vortex structure provided that they have the same global phase shift (Kinsey and Dumas, 2012b). A global phase shift near 90° results in an increased performance in the downstream wing.

An investigation by Liu et al. (2013) on a parallel twin-foil configuration for various nominal effective AoA's shows much higher energy generation than a single foil. This is attributed to a relatively small gap between the two foils, which enriches the vortex interactions and improves the energy extraction ability.

4. Review on semi-activated systems

Compared to forced oscillating motions we discussed above, the semi-activated system promises a more feasible approach in practice. These devices are usually characterized by a prescribed pitching but with a free heaving motion.

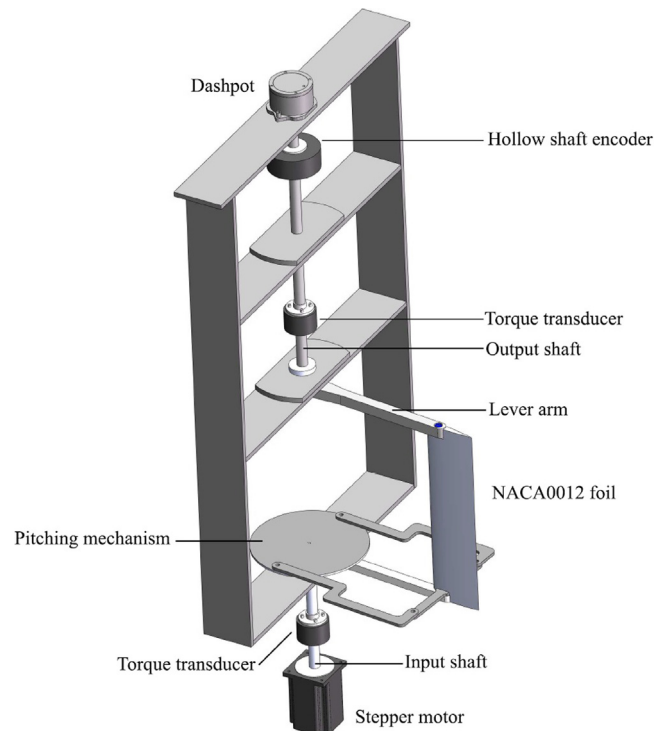


Fig. 9. A laboratory-scale model of a semi-activated flow-energy harvesting device (Huxham, 2012).

Specifically, in this design, the pitching motion is activated so that the angle of attack varies periodically. The resulting oscillation in lifting force generates a periodic heaving motion, from which energy extraction can be achieved. For simplicity, in the mathematical model the electric generator is often idealized as a linear damper attached to the heaving motion. Such a system requires an activating/controlling device and subsequent power input to generate the pitching motion. Positive energy extraction is achieved if the average power extraction from the heaving motion is higher than the energy expenditure for pitching. In fact, this is the principle adapted by an early full-size experimental device, a 150 kW system called ‘Stingray’ developed by Engineering Business Ltd. in UK. This device includes a single hydrofoil with a span of 15.5 m and a chord of 3 m installed in the Shetland Islands, UK. In the design process of Stingray quasi-static representation of fluid dynamic forcing was applied. The energy extraction efficiency of the system, however, remains far below the theoretically predicted peaks based on prescribed heave/pitch motions.

To explore the performance of a semi-activated system at different combinations of parameters, several numerical models have been developed to study the underlying fluid–structure interaction mechanisms. By assuming that the resultant heaving motion is sinusoidal, Shimizu et al. (2008) employed optimization algorithms based on two-dimensional Navier–Stokes solutions and showed that low frequency large amplitude heaving motions generated large power extraction, whereas high frequency small amplitude motions lead to high efficiency.

Fully coupled fluid–structure interaction studies have also been conducted by using a two-dimensional thin-plate model and a three-dimensional boundary-element model (Zhu et al., 2009). These models are based on the potential-flow framework, which is restricted to small effective angles of attack since the effect of LEV is not included. Under these conditions, with sinusoidal pitching motions the maximum power extraction was theoretically predicted as $(\pi/8)\rho c s U_\infty^3 \theta_0^2$. In that study, it was also illustrated that three-dimensional effect associated with small span-to-chord ratios would decrease the energy harvesting efficiency, while ground effect could enhance it.

To take into account the effect of LEV (especially the vorticity control mechanisms that may enhance the performance of the system), this fluid–structure interaction problem is re-examined using a two-dimensional Navier–Stokes model (Zhu and Peng, 2009). Compared with the inviscid models, in CFD simulations the low-pressure area generated by LEV may increase the lifting force and enhance the energy harvesting capacity, whereas the viscous damping may reduce energy extraction. In addition, through vortex–body interactions the energy of the leading-edge vortices can be partially recovered near the trailing edge of the foil, provided that the leading edge separation and the foil motion are correctly synchronized (Fig. 8).

A laboratory experiment was recently conducted in a water tunnel in the University of Sydney by using a small-scale model whose chord length is 0.1 m (Huxham, 2012; Huxham et al., 2012). Similar to Stingray, in this design the device undergoes not a linear heave, but an angular heave motion (Fig. 9). Through systematic tests, it has been demonstrated that the maximum energy harvesting efficiency is around 27%, occurring at the pitching amplitude of 62° and a reduced

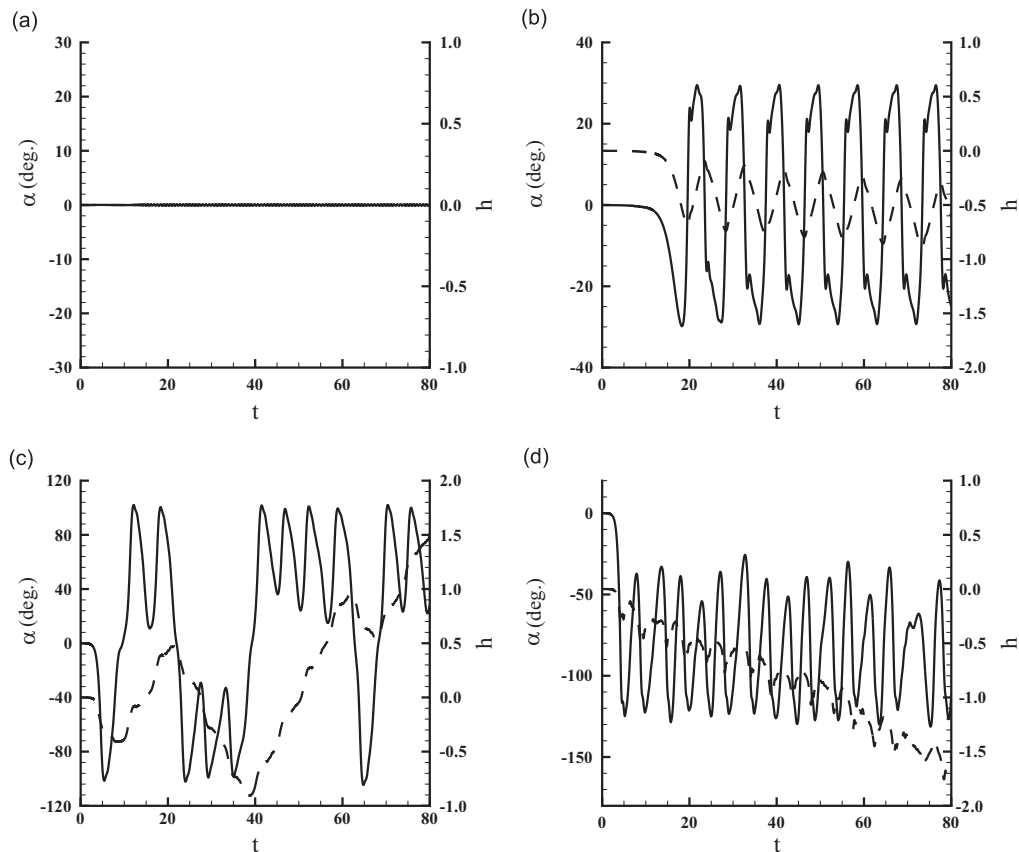


Fig. 10. The four dynamic responses of a foil with free pitch and heave motions: (a) stationary, (b) periodic pitch and heave, (c) chaotic with mode switching, and (d) flip over. α is the pitch angle.

oscillating frequency of 0.1. It is worthwhile to notice that due to mechanical limitation the maximum pitching amplitude in these tests happens to be 62° . The performance of the system beyond that point has not been studied.

5. Review on self-sustained systems

Without the controlling and activation systems to generate the pitching motion, a self-sustaining system provides a mechanically simpler alternative. In such a design the foil is free to respond to the incoming flow in both the pitching and the heaving directions. The underlying principle is similar to self-started and self-sustained fluttering motions of foils (see for example Ghadiri and Razi, 2007; Poirel et al., 2008; Razak et al., 2011). Since the foil is essentially free, it is critical to predict its motion for safe and efficient energy harvesting. Indeed, in fluttering motions both periodic and chaotic responses have been reported (Patil et al., 2001). The chaotic response is not predictable and controllable so that it is not desirable in an energy harvester.

To investigate the possibility and requirement to achieve periodic self-sustained foil responses for high-efficiency energy harvesting, a numerical study has been conducted by using a fully coupled fluid-structure interaction model based on a two-dimensional Navier–Stokes solver (Peng and Zhu, 2009). This study focused on a simple design in which the foil is mounted on a base consisting of a torsional spring in pitch and a linear damper in heave (representing the generator). An interesting finding is that the location of the pitch axis plays a pivotal role in determining the dynamics of the system. Specifically, depending on this factor as well as the strength of the torsional spring, four different dynamic behaviors have been identified (Fig. 10): Response I. Stationary response, which occurs when the pitch axis is close to the leading edge or the rotational spring is sufficiently strong so that the foil remains stationary; Response II. Periodic pitch and heave motions; Response III. Chaotic responses during which the foil switches between two quasi-periodic modes; Response IV. Flip over, which occurs when the pitch axis is close to the trailing edge. Among these response modes, Response 2 is the most desirable for energy harvesting due to its predictability and controllability.

Further studies have been carried out to examine the energy performance of this system in Response 2. It was found that at certain combinations of torsional spring stiffness and pitch axis location, the dominant response frequency (the reduced frequency) approaches 0.12–0.15, the optimal frequency for energy harvesting. The corresponding peak value of energy harvesting efficiency is around 20% (at a Reynolds number of 1000).

Table A1

Investigators	Analysis type	Foil number	Foil cross-section	Operation configuration	AR	Re	f^*	Plunging motion profile	ϕ_{1-2} (deg)	X/c	φ (deg)	h_0/c	θ_0/α_0 (deg)	Pivot location	Efficiency
Ashraf et al. (2011)	CFD	1	NACA 0014	–	2D	20 000	0.8	Sinusoidal and non-sinusoidal	–	–	70–130	1.05	$\theta_0=70$ – 130	1/2	Max $\eta=34\%$ at non-sinusoidal; $\varphi=90^\circ$ 20% Efficiency reduction but a better self-starting and self-driving ability $\eta=32$ – 37% at $U_\infty=1$ m/s
		2		Tandem											
Abiru and Yoshitake (2011)	Experiment	1	NACA 0015	–	3	60 000–120 000	0.3	Induced	–	–	90	0.19–0.7	$\theta_0=30$, 45 and 50	1/2	
Campobasso and Drofelnik (2012)	CFD	1	NACA 0015	–	2D	1100	0.14 and 0.18	Sinusoidal	–	–	90	1	$\theta_0=60$ and 76.33	1/3	Max $\eta=35\%$
Dumas and Kinsey (2006)	CFD		NACA 0015		2D	500, 1100, 2400	0.12–0.18				90	1.0, 1.5	$\theta_0=70$ – 80	1/3	
Davids (1999)	Numerical simulation	1	NACA0012	–	2D	28 000–46 000	0.25–2.5	Sinusoidal	–	–	60–130	0.1–2.0	$\theta_0=7.71$ – 76.31	–0.3–1.3	$\eta=30.03\%$ at $f^*=1.975$, $h_0/c=0.625$, pivot location =0.55, $\theta_0=94$
	Experiment				5.6		0.115–1.187				69.43–105.43	0.5264–0.8439	$\theta_0=35.5$ – 105.43	0.41 and 0.51	
Huxham et al. (2012)	Experiment	1	NACA 0012	–	3.4	45 000	0.025–0.2	Induced	–	–		Up to 1	$\theta_0=4$ –62	1/4	Max $\eta=23.8\%$ at $\alpha_0=58$; $f^*=0.1$
Jones and Platzer (1997)	Numerical simulation	1	NACA0012	–	2D	∞	0.1–20	Sinusoidal	–	–	70–160	0.2	$\theta_0=0$ –15	1/4	
Jones et al. (1999)	Numerical simulation	2	Helicopter rotor blade	Tandem											
	Experiment	1		–	5.6	Up to 30 000	1.5–2.5	Sinusoidal	–	–	90	0.3	$\theta_0=25$ and 30	1/2	Max $\eta=0.26$ at $\alpha_0=15$, $f^*=1.6$, $h_0/c=0.95$
Jones et al. (2003)	Exp and simulation		NACA0014	Tandem	CFD 2D; exp 5.4	20 000 (laminar); 1 000 000 (turbulent) and 22 000	0.2–1.2; 0.65–0.98	Sinusoidal		9.6	80, 90, 100 and 110	1.3 and 1.4	$\theta_0=73$	1/4	
Kinsey and Dumas (2008)	CFD	1	NACA0015	–	2D	1100	0.06–0.2	Sinusoidal	–	–	90	0–1.5	$\theta_0=20$ – 80	1/3	Max η at $f^*=0.75$ – 1.1 , $\alpha_0=70$ – 80
Kinsey et al. (2011)	Experiment	2	NACA 0015	Tandem	7	480 000	0.12	Sinusoidal	180	5.4	90	1	$\theta_0=75$	1/3	Max $\eta=40\%$
Kinsey and Dumas (2012a)	CFD	1	NACA0015	–	7.0 (for 3D)	500 000	0.04–0.2	Sinusoidal	–	–	90	1	$\theta_0=75$	1/3	Max $\eta=40\%$ at $f^*=0.16$
		2		Tandem											
Kinsey and Dumas (2012b)	CFD	2	NACA0015	Tandem	2D	500 000	0.04–0.2	Sinusoidal	90 and 180	3.6–7.5	90	0.75 and 1	$\theta_0=62$ – 75	1/3	Max $\eta=65\%$
Kinsey and Dumas (2012c)	CFD	1	NACA0015	–	5–10	500 000	0.14	Sinusoidal	–	–	90	1	$\theta_0=75$	1/3	

Table A1 (continued)

Investigators	Analysis type	Foil number	Foil cross-section	Operation configuration	AR	Re	f^*	Plunging motion profile	ϕ_{1-2} (deg)	X/c	φ (deg)	h_0/c	θ_0/α_0 (deg)	Pivot location	Efficiency
Lindsey (2002)	Experiments	2	NACA0010; NACA0014 and NACA0018	Tandem	5.4	1 000 000 and 20 000	0.8, 1.0 and 1.3	Sinusoidal	90	4.8	80–110	1, 1.3, 2 and 2.1	$\alpha_0=10-20$	12.5–80%	Max η at $\phi_{1-2}=90$; $\alpha_0=20$
	Numerical simulation														
Le et al. (2013)	CFD	1	NACA 0008; NACA 0012 and scallop shell shape foil	–	2D	90 000	0.1–0.15	Sinusoidal	–	–	90	0.667–1.1	$\theta_0=55-65$	1/3	
Liu et al. (2013)	CFD	1	NACA 0012	–	2D	1 000 000	0.05–0.25	Sinusoidal	–	–	90	0.5 and 1.0	$\alpha_0=0, 5$ and 10	1/3	7.68% efficiency increase
		2		Parallel					180	2 and 3					
McKinney and DeLaurier (1981)	Analytical and wind tunnel test		NACA0012			85 000–110 000	0.39–0.71					0.3	$\theta_0=25-30$	1/2	
Platzter and Bradley (2009)	Experiment	1	–	–							90		$\theta_0=50-80$	1/2	
Platzter et al. (2010)	Experiment	1	NACA 0014	–	2.133	20 000	0.8	Sinusoidal	–	–	90	1.05	$\theta_0=73$	1/2	Max $\eta=33\%$
Simpson et al. (2008a)	CFD	1	NACA 0012	–	4.1, 5.9 and 7.9	13 800	0.2–0.6	Sinusoidal	–	–	90	1.23	$\theta_0=11-57$	1/4	Max $\eta=57\%$
Simpson et al. (2008b)	Experiment	1	NACA 0012	–	4.1, 5.9 and 7.9	13 800	0.2–0.6	Sinusoidal	–	–	90	1.23	$\theta_0=11-57$	1/4	Max $\eta=57\%$
Usoh et al. (2012)	CFD	1	NACA 0012 & non-profiled plate	–	2D	1100	0.6–1.2	Sinusoidal	–	–	90	1	$\theta_0=50-90$	1/3	Max $\eta=34.23\%$ at $f^*=0.80$ and $\theta_0=75$
Xiao et al. (2012)	CFD	1	NACA0012	–	2D	10 000	0.05–0.45	Sinusoidal & Non-sinusoidal	–	–	90	0.5, 1.0	$\alpha_0=10,20$	1/3	Max $\eta=50\%$
Zhu (2011)	Numerical simulation	1	Joukowski foil	–	–	100–1000	0.06–0.2	Sinusoidal	–	–	90	0.5–2.0	$\theta_0=30$ and 90	0.35 and 0.5	Max $\eta=20\%$
Zhu and Peng (2009)	Numerical simulation	1	Joukowski foil	–	2D	1000	–	Induced	–	–	–	–	$\theta_0=15$ and 45	1/3	
Zhu et al. (2009)	Numerical Simulation	1	NACA 0005 and NACA 0025	–	2–10	∞	–	Induced	–	–	–	–	$\theta_0=10-30$	0; 0.25; 0.5; 0.75 and 1	Max η is $\pi\rho\alpha S U^3 \theta^2/8$
Zhu (2012)	Numerical Simulation	1	Joukowski foil	–	2D	1000	–	Induced	–	–	–	–			

^a Nomenclature: **AR**: aspect ratio; f^* : reduced frequency; ϕ_{1-2} : phase shift between two foils; **X**: stream-wise gap between the two foils; **c**: chord length; φ : phase angle between pitching and heave; h_0 : heaving amplitude; θ_0 : pitching amplitude; α_0 : nominal effective angle of attack; U_∞ : incoming flow velocity; η : energy extraction efficiency.

An important limitation of existing studies on flapping foil energy harvester is that they all assume that the incoming flow is uniform and steady, which is likely an oversimplification. Actual flow fields, e.g. rivers or tidal currents, are often non-uniform and sometimes unsteady. While these effects may cause variations in the power extraction of the semi-activated systems, the influence on the self-sustaining systems may be more profound since the response patterns may be changed. To study these effects, in a recent study the dynamics of a self-sustained system similar to the aforementioned one in a linear shear flow has been investigated (Zhu, 2012). Three of the previous response modes, Responses II, III, and IV, remain unchanged. Two additional responses have also been discovered. One of them is a tumbling motion in which the foil rotates around its pitching axis. The other is an irregular motion with no apparent mode competition. In the parametric space, Response II (i.e. the periodic heave/pitch response mode ideal for energy harvesting) still occupies a significantly large area, suggesting that reliable energy harvesting is achievable in linear shear flows. The energy harvesting efficiency can reach 20% at $Re = 1000$.

6. Conclusions and discussion

The development of oscillating wing devices has sparked interest in improving understanding of their underlying physical mechanisms associated with fluid mechanics and fluid–structure interactions. The flow around oscillating foils involves three-dimensional transition to turbulence and flow separation associated with large-scale vortex structure due to unsteady motions; these complex flows are difficult to deal with computationally and experimentally. Due to the limited knowledge on this complex problem, current engineering design approaches generally employ quasi-steady analysis based on reduced fluid dynamics models. As a consequence, there is considerable uncertainty about the unsteady loads on the wings, particularly at large angles of attack. This means that current designs have to be engineered with conservative safety margins, which leads to higher capital costs whilst control strategies are sub-optimal, resulting in reduced energy extraction.

On the other hand, the research on the dynamic behavior of oscillating foil energy extraction devices is in its infancy. The majority of the studies are focused on single wing devices with low Reynolds number. Most simulations are also limited to two-dimensional flows due to the complexities of three-dimensional modeling. This differs significantly from commercial applications which may utilize multiple wings for better performance, use moderate aspect ratio wings, and work in turbulence regime. Moreover, the existing studies are mostly about systems with prescribed pitching/heaving motions. The semi-activated systems and self-sustained systems have not been explored extensively. The existing investigations are mostly about the physics involved while parametric studies are needed.

In terms of energy harvesting efficiency, existing studies have shown that with prescribed sinusoidal motions this oscillating harvester can achieve a maximum efficiency around 30% in small to intermediate Reynolds numbers (around 1000). With prescribed non-sinusoidal oscillating, an increased efficiency as large as 40–50% is reachable. Other efficiency-enhancing measures include corrugations at foil surface, structural flexibility, and multiple foil systems, have also been explored. With semi-activated or self-sustained systems, the peak efficiency is slightly lower (around 20%) (Zhu and Peng, 2009; Peng and Zhu, 2009). One interesting trend is the dependence of energy harvesting efficiency upon Reynolds number. It has been illustrated that as Reynolds number increases the efficiency may also increase (Lindsey, 2002; Jones et al., 2003; Dumas and Kinsey, 2006; Kinsey and Dumas, 2008; Zhu, 2011). The implication is that in real applications the achievable efficiency may be even higher than predications by numerical simulations and laboratory-scale experiments due to high Reynolds numbers.

To pave the way for the development of high performance systems with commercial applications, we envisage the following critical directions for experimental and numerical studies in the near future: (1) deeper explorations of three-dimensional effects and high-Reynolds number effects; (2) fully coupled fluid–structure interaction studies to investigate not only the semi-activated and self-sustained systems but also the effect of the structural deformability of the foil itself; and (3) systematic studies of the coupled dynamics including the fluid loading, the structural response, and a comprehensive model of the energy generator (rather than the idealized linear dampers used in most existing work). Specifically, the efficiency of the mechanical system and the electricity-converter should be considered.

The main objective of this paper is to review the latest research on oscillating wing tidal energy devices; however, it is worthy to note that there are several other types of oscillating energy devices that are similar in principle to the flapping foil harvesters. These include VIVACE (Vortex Induced Vibration Aquatic Clean Energy), a flow energy extractor that utilizes vortex induced vibrations of cylinders (Bernitsas et al., 2006; Raghavan and Bernitsas, 2011) and piezoelectric membrane devices mentioned earlier (Tang et al., 2009; Doaré and Michelin, 2011; Michelin and Doaré, 2013). With this in mind, we anticipate that in the near future, more innovative oscillating-type renewable energy devices may be developed and brought to the commercial market.

Appendix A. A.1. Summary of past computational and experimental studies of undulation foil

See Table A1.

References

- Ashraf, M.A., Young, J., Lai, J.C.S., Platzer, M.F., 2011. Numerical analysis of an oscillating-wing wind and hydropower generator. *AIAA Journal* 49 (7), 1374–1386.
- Abiru, H., Yoshitake, A., 2011. Study on a flapping wing hydroelectric power generation system. *Journal of Environmental Engineering* 6, 178–186.
- Belyayev, V.V., Zuyev, G.V., 1969. Hydrodynamic hypothesis of schooling in fish. *Journal of Ichthyology* 9, 578–584.
- Bernitsas, M.M., Raghavan, K., Ben-Simon Y., Garcia, E.M.H., 2006. VIVACE (Vortex Induced Vibration for Aquatic Clean Energy): a new concept in generation of clean and renewable energy from fluid flow, OMAE06-92645. In: Proceedings of 25th International OMAE Conference, June 4–9, 2006, Hamburg, Germany.
- Campobasso, M.S., Drofelnik, J., 2012. Compressible Navier–Stokes analysis of an oscillating wing in a power-extraction regime using efficient low-speed preconditioning. *Computers and Fluids* 67, 26–40.
- Deng, J., Shao, X.M., Yu, Z.S., 2007. Hydrodynamic studies of two wavy foils in tandem arrangement. *Physics of Fluids* 19, 113104.
- Doaré, O., Michelin, S., 2011. Piezoelectric coupling in energy-harvesting fluttering flexible plates: linear stability analysis and conversion efficiency. *Journal of Fluids and Structures* 27, 1357–1375.
- Dumas, G., Kinsey, T., 2006. Eulerian simulations of oscillating airfoils in power extraction regime. In: Rahman, Brebbia (Eds.), Proceedings in Advances in Fluid Mechanics VI, WIT Press, pp. 245–254.
- Davids, S.T., 1999. A Computational and Experimental Investigation of a Flutter Generator. Master thesis. Department of Aeronautics and Astronautics, Naval Postgraduate School.
- Ghadiri, B., Razi, M., 2007. Limit cycle oscillations of rectangular cantilever wings containing cubic nonlinearity in an incompressible flow. *Journal of Fluids and Structures* 23 (4), 665–680.
- Grue, J., Mo, A., Palm, E., 1988. Propulsion of a foil moving in water waves. *Journal of Fluid Mechanics* 186, 393–417.
- Huxham, G., 2012. Experimental Investigation of an Oscillating Foil Tidal Stream Energy Converter. Master thesis. The University of Sydney.
- Huxham, G., Cochard, S., Patterson, J., 2012. Experimental parametric investigation of an oscillating hydrofoil tidal stream energy converter. In: Proceedings of 18th Australasian Fluid Mechanics Conference AFMC 2012. Australasian Fluid Mechanics Society, Launceston, Tasmania.
- Isshiki, H., Murakami, M., 1984. A theory of wave devouring propulsion. *Journal of Society of Naval Architecture Japan* 156, 102–114.
- Jones, K.D., Platzer, M.F., 1997. Numerical Computation of Flapping-wing Propulsion and Power Extraction. AIAA Paper 97-0826.
- Jones, K.D., Davids S.T., Platzer, M.F., 1999. Oscillating-wing power generation. In: Proceedings of 3rd ASME/SME Joint Fluids Engineering Conference.
- Jones, K.D., Lindsey, K., Platzer, M.F., 2003. An investigation of the fluid–structure interaction in an oscillating-wing micro-hydropower generator. *Fluid Structure Interaction II*, vol. 2. WIT Press, Southampton, England, UK73–82.
- Katz, J., Weihs, D., 1978. Hydrodynamic propulsion by large amplitude oscillation of an airfoil with chordwise flexibility. *Journal of Fluid Mechanics* 88 (3), 485–497.
- Kerr, D., 2007. Marine energy. *Philosophical Transactions of the Royal Society A* 365, 971–992.
- Kesel, A.B., 2000. Aerodynamic characteristics of dragonfly wing sections compared with technical aerofoils. *Journal of Experimental Biology* 203, 3125–3135.
- Kinsey, T., Dumas, G., 2008. Parametric study of an oscillating airfoil in a power-extraction regime. *AIAA Journal* 46 (6), 1318–1330.
- Kinsey, T., Dumas, G., Lalande, G., Ruel, J., Mehut, A., Viarogue, P., Lemay, J., Jean, Y., 2011. Prototype testing of a hydrokinetic turbine based on oscillating hydrofoils. *Renewable Energy* 36, 1710–1718.
- Kinsey, T., Dumas, G., 2012a. Computational fluid dynamics analysis of a hydrokinetic turbine based on oscillating hydrofoils. *Journal of Fluids Engineering* 134 (2), 021104.
- Kinsey, T., Dumas, G., 2012b. Optimal tandem configuration for oscillating-foils hydrokinetic turbine. *Journal of Fluids Engineering* 134 (3), 031103.
- Kinsey, T., Dumas, G., 2012c. Three-dimensional effects on an oscillating-foil hydrokinetic turbine. *Journal of Fluids Engineering* 134, 071105.
- Langhamer, O., Haikonen, K., Sundberg, J., 2010. Wave power – sustainable energy or environmentally costly? A review with special emphasis on linear wave energy converters. *Renewable and Sustainable Energy Reviews* 14, 1329–1335.
- Le, T.Q., Ko, J.H., Byun, D.Y., 2013. Morphological effect of a scallop shell on a flapping-type tidal stream generator. *Bioinspiration and Biomimetics* 8, 036009.
- Lefrançois, J., 2008. Optimisation de rendement d'une turbine multi-ailes à l'aide d'une méthode lagrangienner par particules vortex. M.S. thesis. Laval University, Quebec City, Canada.
- Liao, J.C., Beal, D.N., Lauder, G.V., Triantafyllou, M.S., 2003. Fish exploiting vortices decrease muscle activity. *Science* 302, 1566–1569.
- Licht, S., Wibawa, M., DeLaurier, J., 1981. The wingmill: an oscillating-wing wind-mill. *Journal of Energy* 5, 109–115.
- Michelin, S., Stefan, G., Llewellyn, S., 2009. Resonance and propulsion performance of a heaving flexible wing. *Physics of Fluids* 21, 071902.
- Michelin, S., Doaré, O., 2013. Energy harvesting efficiency of piezoelectric flags in axial flows. *Journal of Fluid Mechanics* 714, 489–504.
- Patil, M.J., Hodges, D.H., Cernik, C.E.S., 2001. Limit-cycle oscillations in high-aspect-ratio wings. *Journal of Fluids and Structures* 15 (1), 107–132.
- Peng, Z., Zhu, Q., 2009. Energy harvesting through flow-induced oscillations of a foil. *Physics of Fluids* 21, 123602.
- Platzer, M.F., Bradley, R.A., 2009. Oscillating-wing power generator with flow-induced pitch-plunge phasing. IPC8 Class: AF03D900FI USPC Class: 290 55 US Patent.
- Platzer, M., Ashraf, M., Young, J., Lai, J., 2010. Extracting power in jet streams: pushing the performance of flapping wing technology. In: 27th Congress of the International Council of the Aeronautical Sciences. International Council of the Aeronautical Sciences Paper 2010-2.9.1. September 19–24, 2010, Nice, France.
- Poirel, D., Harris, Y., Benaissa, A., 2008. Self-sustained aeroelastic oscillations of a NACA0012 airfoil at low-to-moderate Reynolds numbers. *Journal of Fluids and Structures* 24 (5), 700–719.
- Raghavan, K., Bernitsas, M.M., 2011. Experimental investigation of Reynolds number effect on vortex induced vibration of rigid circular cylinder on elastic supports. *Ocean Engineering* 38 (5–6), 719–731.
- Ramanarivo, S., Godoy-Diana, R., Thiria, B., 2011. Rather than resonance, flapping wing flyers may play on aerodynamics to improve performance. Proceedings of the National Academy of Sciences 108, 1017910108.
- Razak, N.A., Andrianne, T., Dimitriadis, G., 2011. Flutter and stall flutter of a rectangular wing in a wind tunnel. *AIAA Journal* 49 (10), 2258–2271.
- Simpson B.J., Hover, F.S., Triantafyllou, M.S., 2008a. Experiments in direct energy extraction through flapping foils. In: Proceedings of the Eighteenth International Offshore and Polar Engineering Conference. July 6–11, 2008, Canada.
- Simpson, B.J., Licht, S., Hover, F.S., Triantafyllou, M.S., 2008b. Energy extraction through flapping foils. In: Proceedings of 27th International Conference on Offshore Mechanics and Arctic Engineering, OMAE-2008-58043.
- Shimizu, E., Isogai, K., Obayashi, S., 2008. Multiobjective design study of a flapping wing power generator. *Journal of Fluids Engineering* 130, 021104.
- Shoele, K., Zhu, Q., 2013. Performance of a wing with nonuniform flexibility in hovering flight. *Physics of Fluids* 25, 041901.
- Tang, L., Paidoussis, M.P., Jiang, J., 2009. Cantilevered flexible plates in axial flow: energy transfer and the concept of flutter-mill. *Journal of Sound and Vibration* 326 (1), 263–276.
- The Engineering Business Ltd., 2002. Stingray Tidal Stream Energy Device – Phase 1. Technical Report.

- The Engineering Business Ltd., 2003. Stingray Tidal Stream Energy Device – Phase 2. Technical Report.
- The Engineering Business Ltd., 2005. Stingray Tidal Stream Energy Device – Phase 3. Technical Report.
- Thiria, B., Godoy-Diana, R., 2010. How wing compliance drives the efficiency of self-propelled flapping flyers. *Physical Review E* 82, 015303.
- Triantafyllou, M.S., Triantafyllou, G.S., Gopalkrishnan, R., 1991. Wake mechanics for thrust generation in oscillating foils. *Physics of Fluids A* 3, 2835–2837.
- Triantafyllou, G.S., Triantafyllou, M.S., Grosenbaugh, M.A., 1993. Optimal thrust development in oscillating foils with application to fish propulsion. *Journal of Fluids and Structures* 7, 205–224.
- Triantafyllou, M.S., Techet, A.H., Hover, F.S., 2004. Review of experimental work in biomimetic foils. *IEEE Journal of Ocean Engineering* 29, 585–594.
- Usoh, C.O., Young, J., Lai, J.C.S., Ashraf, M.A., 2012. Numerical analysis of a non-profiled plate for flapping wing turbines. In: *Proceedings of the 18th Australasian Fluid Mechanics Conference*, Launceston, Australia.
- Westwood, A., 2004. Ocean power wave and tidal energy review. *Refocus* 5, 50–55.
- Wu, T.Y., 1972. Extraction of flow energy by a wing oscillating in waves. *Journal of Ship Research* 16, 66–78.
- Wu, T.Y., Chwang, A.T., 1975. Extraction of flow energy by fish and birds in a wavy stream. In: *Proceedings of the Symposium on Swimming and Flying in Nature*. Plenum Press, New York.
- Xiao, Q., Liao, W., Yang, S.C., Peng, Y., 2012. How motion trajectory affects energy extraction performance of a biomimic energy generator with an oscillating foil? *Renewable Energy* 37, 61–75.
- Yin, B., Luo, H., 2010. Effect of wing inertia on hovering performance of flexible flapping wings. *Physics of Fluids* 22, 111902.
- Zhu, Q., Wolfgang, M., Yue, D.K.P., Triantafyllou, M.S., 2002. Three-dimensional flow structures and vorticity control in fish-like swimming. *Journal of Fluid Mechanics* 468, 1–28.
- Zhu, Q., 2007. Numerical simulation of a flapping foil with chordwise or spanwise flexibility. *AIAA Journal* 45 (10), 2448–2457.
- Zhu, Q., Peng, Z., 2009. Mode coupling and flow energy harvesting by a flapping foil. *Physics of Fluids* 21 (3), 033601.
- Zhu, Q., Haase, M., Wu, C.H., 2009. Modeling the capacity of a novel flow-energy harvester. *Applied Mathematical Modelling* 33 (5), 2207–2217.
- Zhu, Q., 2011. Optimal frequency for flow energy harvesting of a flapping foil. *Journal of Fluid Mechanics* 675, 495–517.
- Zhu, Q., 2012. Energy harvesting by a purely passive flapping foil from shear flows. *Journal of Fluids and Structures* 34, 157–169.